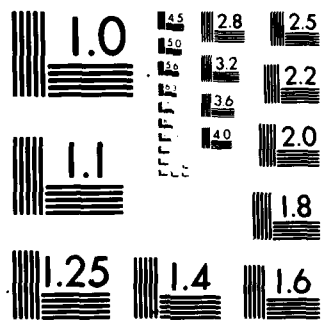END
DATE
FILMED
8-80
DTIC

MICROCOPY RESOLUTION TEST CHART
NATIONAL BUREAU OF

/5'

LEVEL Ⅱ

⑫

ADA086703

Theoretical Antenna Analyses

H. E. KING, R. B. DYBDAL, and D. S. CHANG
Electronics Research Laboratory
Laboratory Operations
The Aerospace Corporation
El Segundo, Calif. 90245

1 July 1980

DTIC
SELECTED
JUL 1 6 1980
E

Interim Report

DDC FILE COPY

This interim report was submitted by The Aerospace Corporation, El Segundo, Calif. 90245, under Contract No. F04701-79-C-0080 with the Space Division, Contracts Management Office, P.O. Box 92960, Worldway Postal Center, Los Angeles, Calif. 90009. It was reviewed and approved for The Aerospace Corporation by M. T. Weiss, Acting Director, Electronics Research Laboratory. Gerhard E. Aichinger was the project officer for Mission-Oriented Investigation and Experimentation (MOIE) Programs.

This report has been reviewed by the Public Affairs Office (PAS) and is releasable to the National Technical Information Service (NTIS). At NTIS, it will be available to the general public, including foreign nations.

This technical report has been reviewed and is approved for publication. Publication of this report does not constitute Air Force approval of the report's findings or conclusions. It is published only for the exchange and stimulation of ideas.

Gerhard E. Aichinger
Project Officer

FOR THE COMMANDER

Evan R. Brossman, Chief
Contracts Management Office

SECURITY CLASSIFICATION OF THIS PAGE (When Data Entered)

REPORT DOCUMENTATION PAGE	READ INSTRUCTIONS BEFORE COMPLETING FORM

1. REPORT NUMBER	2. GOVT ACCESSION NO.	3. RECIPIENT'S CATALOG NUMBER
SD-TR-80-50	AD-A086703	

4. TITLE (and Subtitle)	5. TYPE OF REPORT & PERIOD COVERED
THEORETICAL ANTENNA ANALYSES	Interim rept.
	6. PERFORMING ORG. REPORT NUMBER
	TR-0080(5930-06)-1

7. AUTHOR(s)	8. CONTRACT OR GRANT NUMBER(s)
H. E. King Robert B. Dybdal and Dorothy S. Chang	F04701-79-C-0080

9. PERFORMING ORGANIZATION NAME AND ADDRESS	10. PROGRAM ELEMENT, PROJECT, TASK AREA & WORK UNIT NUMBERS
The Aerospace Corporation El Segundo, Calif. 90245	

11. CONTROLLING OFFICE NAME AND ADDRESS	12. REPORT DATE
Space Division Air Force Systems Command Los Angeles, Calif. 90009	1 July 1980
	13. NUMBER OF PAGES
	22

14. MONITORING AGENCY NAME & ADDRESS(if different from Controlling Office)	15. SECURITY CLASS. (of this report)
	Unclassified
	15a. DECLASSIFICATION/DOWNGRADING SCHEDULE

16. DISTRIBUTION STATEMENT (of this Report)

Approved for public release; distribution unlimited

17. DISTRIBUTION STATEMENT (of the abstract entered in Block 20, if different from Report)

18. SUPPLEMENTARY NOTES

19. KEY WORDS (Continue on reverse side if necessary and identify by block number)

Antenna Analysis
Diffraction Theory
Edge Diffraction Theory

Monopole Antenna
Parabolic Reflector

20. ABSTRACT (Continue on reverse side if necessary and identify by block number)

The results of the analytical work for the Antennas task of the FY 1979 Mission-Oriented Investigation and Experimentation (MOIE) program are summarized. The radiation pattern computation of a 46.8λ diameter paraboloidal reflector antenna is compared with experimental results. The pattern analysis accounts for the feed blockage and feed-strut scatter. Good agreement between the theoretical and experimental results exists for wide-angle sidelobes. The diffraction levels from a half-plane edge and a rounded edge were computed, and good correlation

DD FORM 1473
(FACSIMILE)

392106

19. KEY WORDS (Continued·)

20. ABSTRACT (Continued)

with experimental results is indicated. The radiation patterns of a monopole mounted on a circular and a rectangular ground plane were also computed.

CONTENTS

1

FIGURES

I. INTRODUCTION

Space Division and the Aerospace program offices have a continuing
requirement to establish the feasibility of new electromagnetic concepts for
space, reentry, air, ground (including hardened terminals), and subterranean
applications. The feasibility of the advanced concepts is established by both
theoretical analyses and experimental studies. The Electronics Research
Laboratory (ERL) develops and maintains experimental facilities required to
investigate new antenna concepts, confirm contractor's antenna designs, and
evaluate the performance of special purpose antennas. A portion of the
Mission-Oriented Investigation and Experimentation (MOIE) program effort is
devoted to the maintainance and upgrading of these experimental facilities in
order to provide the required support.

In recent years, much progress has been made in the development of
practical user-oriented computer analyses capable of examining many types of
antenna systems. An objective of the MOIE program was to utilize such analy-
ses to extend in-house capabilities. The achievement of this objective is
warranted by the increasingly mature technology required of present and future
systems and will improve ERL support to Space Division. During FY 79, theo-
retical analyses of several types of antennas were completed, which included a
study of (1) the radiation patterns of a 92-GHz, 6-in.-diameter (46.8λ) pa-
raboloidal reflector antenna; (2) the diffraction levels from a half-plane
edge as compared to a rounded edge; and (3) the radiation pattern of a
monopole over a finite-size circular and rectangular ground plane. The
theoretical results were verified by experiments for the 6-in.-diameter an-
tenna and measurements of the diffraction from rounded and half-plane edges.

II. THEORETICAL ANTENNA ANALYSES

A general objective of the MOIE Antennas task was to extend in-house capabilities for theoretical analyses of antenna systems, which would increase the effectiveness of ERL support to several Space Division and Aerospace program offices.

During this year, the achievement towards this objective was started with analyses of the following: (1) the radiation patterns of a 92-GHz, 6-in.-diameter (46.8λ) paraboloidal reflector antenna; (2) the diffraction levels from a half-plane edge as compared to a rounded edge; and (3) the radiation pattern of a monopole over a finite-size circular and rectangular ground plane.

The first analysis was performed because low-sidelobe, high-gain antennas are becoming increasingly important for future system designs. For a thorough understanding of the antenna mechanisms that contribute to the antenna sidelobe energy, we carried out a detailed radiation pattern analysis. One of the most common types of antennas is the paraboloidal reflector with feed struts. Although the antenna has been used in many systems, the wide-angle sidelobes and backlobes have not been thoroughly analyzed until recently; the analyses commonly used in earlier effects are valid for only the main beam region. An existing 6-in.-diameter reflector antenna that was experimentally measured at 92 GHz was chosen for the theoretical analysis. The sidelobe contribution from the struts, feed horn, and reflector edge can be determined from the computer code. The amplitude and phase characteristics of radiation patterns can be determined for both the principal and crossed linear polarization or circular polarization components over the complete angular space.

The second analysis was performed to demonstrate the advantages of a rounded edge over a half-plane (sharp) edge in the reduction of diffraction levels for low-sidelobe antenna applications. This analysis was developed and confirmed by experimental measurements.

The third analysis studied a monopole located on various-size ground planes. The monopole antenna over a ground plane is a simple configuration that is used in many applications. Edge diffraction contributes significantly to the monopole antenna with a finite ground plane. The capability derived from this analysis was immediately used by a program office to assess the effects of relocation of a monopole antenna on a flat spacecraft surface. The analysis is expected to be useful for many future applications.

A. ANALYSIS OF THE PARABOLOIDAL REFLECTOR ANTENNA

For calculation of the antenna radiation pattern of the 92-GHz, 6-in.-diameter reflector, the OSUPATT computer program (Ref. 1) was obtained from Ohio State University (OSU). The geometric theory of diffraction (GTD) and the aperture-integration theory are utilized in this user-oriented program. Also included in the program are the feed and strut scatter and the calculation of the off-principal plane patterns.

The radiation pattern in the forward direction of a reflector antenna can be calculated by the aperture-field method or by the current distribution method as outlined by Silver (Ref. 2). These methods provide accurate results for the main beam and the close-in sidelobes, but, in general, do not provide accurate results for the wide-angle sidelobes. The OSU staff (Ref. 1) analyzed the wide-angle sidelobes and backlobes by the GTD technique and utilized aperture-integration methods to compute the pattern near the forward-axis direction.

The feed-horn blockage is approximated by the replacement of the feed structure with an equivalent circular or rectangular flat-plate model whose area approximates that of the cross section of the feed structure. The conventional physical optics approach is used by the OSUPATT program to determine the flat-plate scattering, which is combined in a phasor sum to the other pattern contributions. The feed-blockage aperture is assumed to be uniform since it is relatively small compared to the reflector diameter.

The scattering from the feed supports is incorporated in the OSUPATT program to determine the equivalent current line sources of each individual strut (Ref. 3). Only metallic circular struts can be treated. The incident field

8

on the struts is assumed to be only the reflected wave from the reflector; i.e., direct coupling from the feed to the strut is not considered. Only the forward scattered strut fields are used in the pattern computations. The GTD technique is used to determine the equivalent line sources. The phasor sum of the fields from each individual strut results in the total radiation from the feed struts. The scattering from the feed horn and the feed supports is combined with the reflector radiation to obtain the total antenna radiation pattern.

The output of OSUPATT consists of the principal and cross-polarized patterns of the strut scattering, the feed scattering, the reflector and direct feed, and total field (including phase and amplitude). As received, the OSUPATT program was restricted to linearly polarized feed systems, but has been subsequently modified in-house for the analysis of circularly polarized configurations. For linear polarization computations, the program required 27 sec for the computation of four patterns (that contained 1801 points each) and for the plotting of eight graphs. The program represents the best available state-of-the-art computer code for reflector antennas.

The antenna used in the circular reflector calculations is a 92-GHz, 6-in. aperture paraboloid with a diagonal feed horn, as shown in Fig. 1. The antenna is a prime focus configuration that has an $F/D = 1/3$. One strut extends beyond the rim of the reflector. The diagonal horn blockage (0.25 x 0.25 in.) was approximated by a 0.288-in. diameter flat plate. A rectangular waveguide was used on the experimental antenna as the feed strut. Since the program requires a circularly shaped strut, the height (0.141 in.) of the rectangular waveguide was assumed to be the diameter of the circular strut. The plane of the strut coincides with the H plane of the antenna. The angle between the strut and the forward axis is $\beta = 52°$. Principal plane feed patterns (E- and H-planes) were tabulated from values based on measured data and used as an input to the program.

The computed patterns, superimposed on the experimentally measured patterns, are shown in Fig. 2. Since the strut lies in the H plane, the E plane pattern has complete symmetry with respect to the main beam. However, because

9

Fig. 1.   Photograph of 29-GHz, 6-in.-Diameter
          Reflector Antenna with Diagonal
          Horn Feed

of the strut position, the H-plane patterns are asymmetric, as shown in
Fig. 2b. Comparison of the computed and measured patterns leads to the
following conclusions:

1.   The close-in and wide-angle sidelobes agree reasonably well in level
     and angular location.

2.   The sudden drop in sidelobe levels at $\theta \sim 107°$ is caused by the
     shadow boundary.
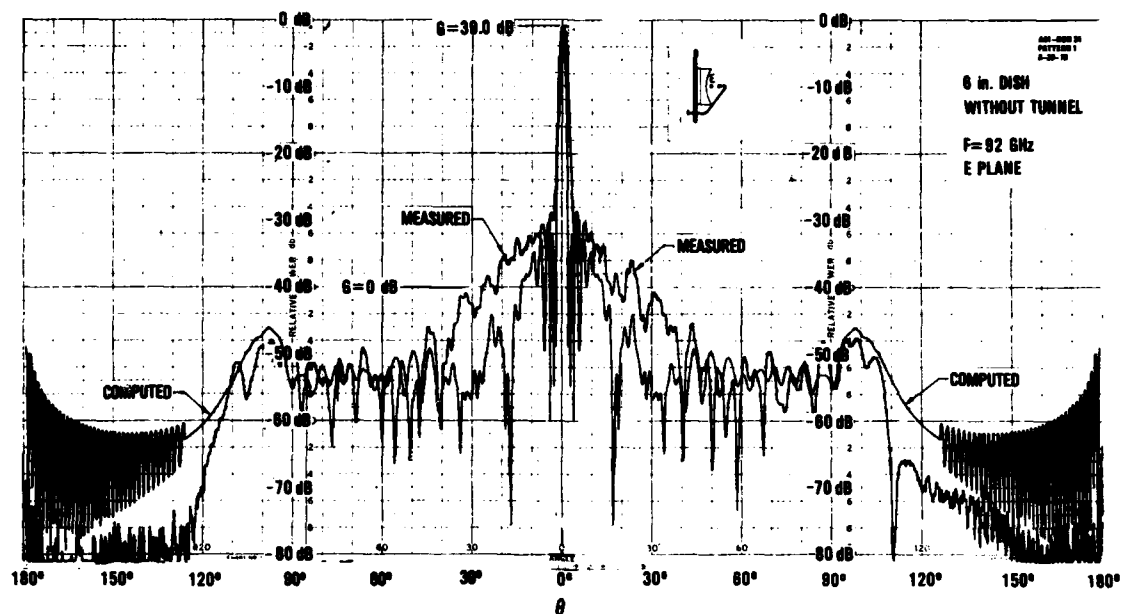
(a)   E Plane
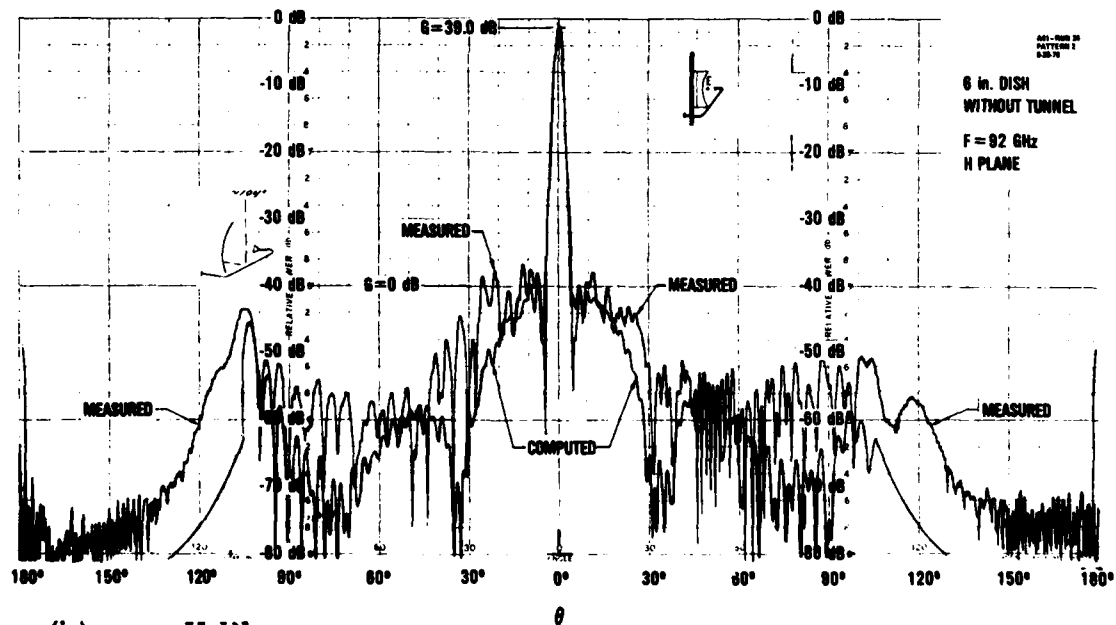
(b)   H-Plane

Fig. 2.   Comparison of Measured and Computed Patterns for a 92-GHz,
          6-in.-Diameter Antenna.   (a) E-plane.   (b) H-plane.

11

3.   The effects of the scattering from the strut are noticeable in the
      H-plane patterns.

The agreement between measured and calculated results is quite remarkable
when the wide dynamic range and some of the differences between the mathemati-
cal and physical models are considered. The dynamic range of these computed
and measured patterns is 80 dB, whereas the conventional dynamic range of
antenna patterns is only 40 dB. A significant amount of effort was expended
to achieve experimentally the dynamic range of the patterns. The repeatabil-
ity of these results even at lower levels was quite good, which is necessary
for valid results. The physical model of the antenna differs from the mathe-
matical model as follows:

1.   The rim of the parabola in the analysis is a sharp edge, whereas the
      actual antenna has a rim with a ~66° wedge angle and a chamfered
      edge, as shown in Fig. 1.

2.   Curved portions of the waveguide are not incorporated in the
      analysis.

3.   The actual antenna has a 12-in.-diameter, absorber-covered disk
      behind it that is not included in the analysis, which results in
      discrepancies in pattern levels primarily in the ~150 to 180°
      angular region.

B.   DIFFRACTED FIELD REDUCTION FROM AN EDGE

A convenient approach to the reduction of the diffracted fields from an
edge is for the edge to be made round. The rounded edge becomes quite effec-
tive when the radius of curvature is significant compared with the wavelength
dimension. Rounded edges are therefore more practical at millimeter wave-
lengths than the microwave regime since a radius large in terms of wavelengths
may be achieved with a modest physical dimension. The mechanisms behind the field
reduction are the lower diffraction from the wave attached to the rounded edge
coupled with the radiation attenuation associated with the creeping wave. An
analysis was completed for the illustration of the improvement in field reduc-
tion from a rounded edge versus a half plane; the geometry for both is given
in Fig. 3. With use of the diffraction coefficients from Kouyoumjian (Refs.
4, 5), the diffracted field from the half-plane and the curved edge is shown
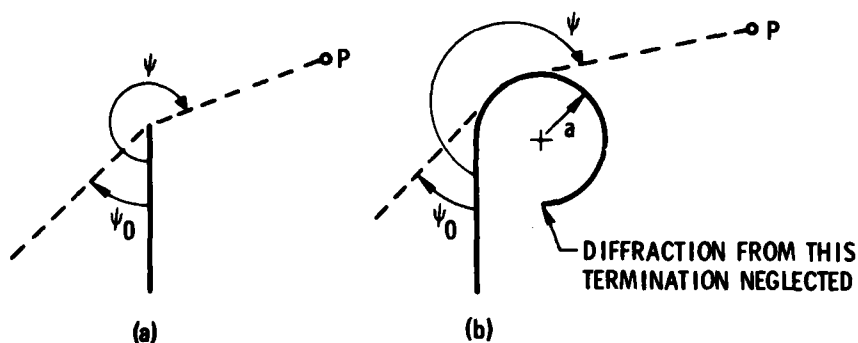in Eqs. (1) and (2), respectively.

Fig. 3. Geometry of a Half-Plane and Rounded Edge for Diffracted Field Reduction. (a) Half-Plane. (b) Rounded edge.

$$|E_d^{hp}| \propto \frac{1}{\sqrt{kr}} \; \frac{1}{2\sqrt{2\pi}} \left[\frac{1}{-\cos\left(\dfrac{\Psi - \Psi_o}{2}\right)} \;\pm\; \frac{1}{-\cos\left(\dfrac{\Psi + \Psi_o}{2}\right)} \right] \tag{1}$$

for the half plane and

$$|E_d^{c}| \propto \frac{1}{\sqrt{kr}} \, (ka)^{1/3} \binom{1.083}{0.644} e^{-\Delta\Psi(ka)^{1/3} \frac{1}{2}\left(2^{2/3}\right)\binom{1.019}{2.338}} \cos\frac{\pi}{6} \tag{2}$$

for the rounded edge,

where $k = 2\pi/\lambda$

$\Delta\Psi = \Psi - \Psi_o$ = angle wave travels around the cylinder

These equations yield the total field in the shadow region. The diffracted field of the rounded edge relative to the half-plane is

13

$$K = \frac{|E_d^c|}{|E_d^{hp}|} = \frac{(ka)^{1/3} \binom{1.083}{0.644} e^{-\Delta\Psi\binom{0.700}{1.607}} (ka)^{1/3}}{0.1995 \left(\dfrac{1}{-\cos\dfrac{\Psi - \Psi_o}{2}} \pm \dfrac{1}{-\cos\dfrac{\Psi + \Psi_o}{2}} \right)} \tag{3}$$

where the upper coefficients and + sign represent the electric field vector E perpendicular to the edge, and the lower coefficients and – sign represent the electric field parallel to the edge.

A representative set of curves that indicates the diffraction reduction for a 30° incidence angle is shown in Fig. 4. The squares and circles represent experimental data points that confirm the analysis quite well.

C. ANALYSIS OF A MONOPOLE OVER A GROUND PLANE

The pattern characteristics of a monopole antenna mounted over a circular or rectangular ground plane can be computed by use of the GTD. This approach was initially discussed in Reference 6, and the diffracted contributions for the circular ground plane were later examined in Reference 7. An analysis was performed in-house so that suitable equations could be obtained for the examination of different ground-plane dimensions. The overall pattern is computed by the addition of the ground-plane edge diffracted components to the monopole direct radiation. The rectangular ground plane can be treated as a two-dimensional problem; the circular ground plane is complicated by the necessity for the consideration of the circumferential edge currents. Integration of the edge currents (Ref. 7) resulted in a relation similar to that of the square ground plane; i.e., the diffraction component was multiplied by $1/\sqrt{\sin\theta}$.

The geometry of the monopole rectangular ground-plane antenna system is shown in Fig. 5. With the use of Reference 6 as a starting point, the radiation pattern equation for the rectangular ground plane may be written as

$$E = \sin\theta + \frac{e^{-j\left[ka_1(1-\sin\theta) + \frac{5\pi}{4}\right]}}{4\pi\sqrt{\dfrac{a_1}{\lambda}}\cos\dfrac{90+\theta}{2}} \pm \frac{e^{-j\left[ka_e(1+\sin\theta) + \frac{\pi}{4}\right]}}{4\pi\sqrt{\dfrac{a_2}{\lambda}}\cos\dfrac{90-\theta}{2}} \tag{4}$$
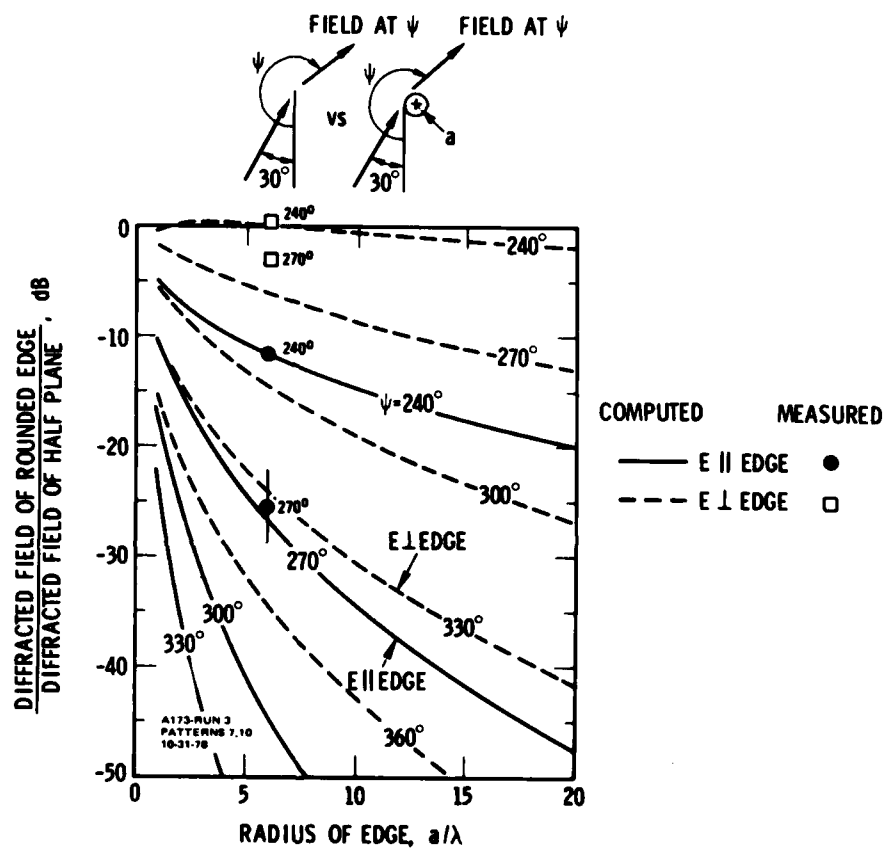
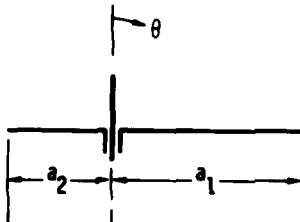Fig. 4. Diffraction Reduction with Rounded Edge
for 30° Incidence Angle

15

Fig. 5. Geometry of Monopole over Rectangular Ground Plane

where $k = 2\pi/\lambda$

λ = wavelength

The $\sin \theta$ term represents the pattern of the monopole on an infinite ground plane and is used only for $0° < \theta < 90°$; i.e., below the ground plane the monopole does not contribute to the overall pattern. The second and third terms represent the diffraction terms from the right and left edges of the ground plane, respectively (see Fig. 5). The + sign is used for the upper hemisphere ($0° < \theta < 90°$) and the − sign is used for the lower hemisphere ($90° < \theta < 180°$).

The diffraction terms of Eq. (4) approach infinity near the shadow boundary region ($\theta \sim 90°$). Rigorous analytical functions are available that result in exact pattern computations near $90°$, but they are not amenable to HP-97 calculator computations. A simpler expansion was used so that values could be obtained near the shadow boundary. The resultant pattern equation is written as

$$E_{SB} = \sin \theta \mp \frac{1}{2}\left(1 - 4\sqrt{\frac{a_1}{\lambda}}\,|\cos\frac{90 + \theta}{2}|\,e^{j\pi/4}\right) \pm \frac{e^{-j\left[ka_2(1 + \sin \theta) + \frac{\pi}{4}\right]}}{4\pi\sqrt{\frac{a_2}{\lambda}}\cos\frac{90 - \theta}{2}} \qquad (5a)$$

for the pattern on the right, and

$$E_{SB} = \sin \theta \pm \frac{e^{-j\left[ka_1 (1 - \sin \theta) + \frac{5\pi}{4}\right]}}{4\pi\sqrt{\frac{a_1}{\lambda}} \cos \frac{90 + \theta}{2}} \pm \frac{1}{2}\left(1 - 4\sqrt{\frac{a_2}{\lambda}} |\cos \frac{90 - \theta}{2}|e^{j\pi/4}\right)$$

(5b)

for the pattern on the left. Again, the sin θ term is used only for the upper hemisphere and is assumed to be zero in the lower hemisphere. The upper signs are used for 0° < θ < 90°; the lower signs, for 90° < θ < 180°. A smoothly drawn curve must be made to join the curves derived from Eqs. (4) and (5) because of the multiply diffracted terms that are not included in the analysis.

A fixed ground-plane length of 5.5λ was selected, and the monopole was located 1λ from the left edge for one computation and at the center of the ground plane for a second computation. The computed patterns are illustrated in Fig. 6. The dashed pattern applies to the monopole located at the center of the ground plane; the solid pattern applies to the monopole off-center. These patterns illustrate the pattern asymmetry that results when the monopole is not centered in the ground plane.
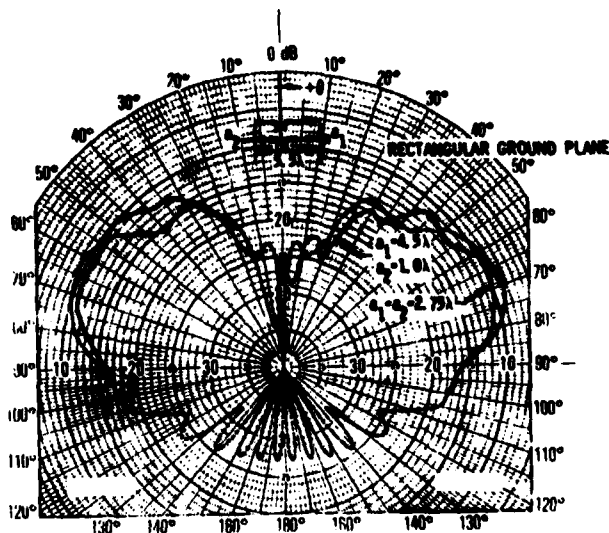

Fig. 6. Computed Patterns of Monopole over 5.5λ
Rectangular Ground Plane

The pattern for a short monopole over a circular ground plane can be expressed by

$$E = \sin\theta + \frac{e^{-j\left[ka(1 - \sin\theta) + \frac{5\pi}{4}\right]}}{4\pi\sqrt{\frac{a}{\lambda}}\,\sin\theta\,\cos\frac{90 + \theta}{2}} \pm \frac{e^{-j\left[ka(1 + \sin\theta) + \frac{\pi}{4}\right]}}{4\pi\sqrt{\frac{a}{\lambda}}\,\sin\theta\,\cos\frac{90 - \theta}{2}} \qquad (6a)$$

$$E_{SB} = \sin\theta \mp \frac{1 - 4\sqrt{\frac{a}{\lambda}}\,|\cos\frac{90 + \theta}{2}|\,e^{j\pi/4}}{2\sqrt{\sin\theta}} \pm \frac{e^{-j\left[ka(1 + \sin\theta) + \pi/4\right]}}{4\pi\sqrt{\frac{a}{\lambda}}\,\sin\theta\,\cos\frac{90 - \theta}{2}} \qquad (6b)$$

where $k = 2\pi/\lambda$

   λ = wavelength,

   a = radius of ground plane

Note that Eqs. (4) and (6) are similar except for the $\sqrt{\sin\theta}$ factor in the denominator of the Eq. (6) diffraction terms. This factor was derived by examination of the asymptotic behavior of the equivalent current diffraction analysis presented in Reference 7. The $\sin\theta$ term for the monopole radiation is used only for the upper hemisphere as it is in the rectangular ground plane antenna system. The upper signs are used for the upper hemisphere, whereas the lower signs are used for the lower hemisphere. Equation (6b) must be used near the shadow boundary. The patterns for a ground plane with a 4.3λ radius are shown in Fig. 7. As a comparison, the pattern of a monopole on a square ground plane whose sides are 8.6λ is shown in Fig. 8. The patterns are similar, except that the circular ground plane pattern produces higher sidelobe levels.

The monopole-ground-plane analysis provides the first step toward the modeling of broad-beam antennas mounted on a spacecraft.
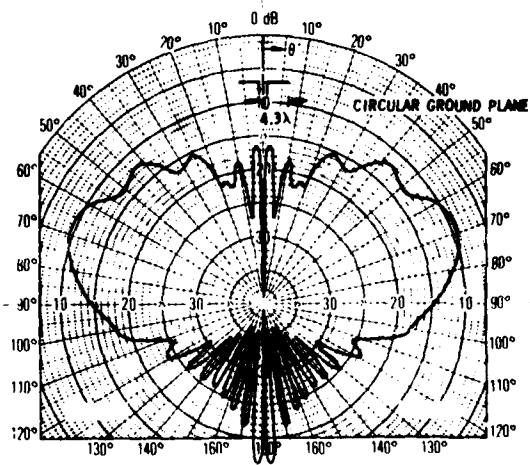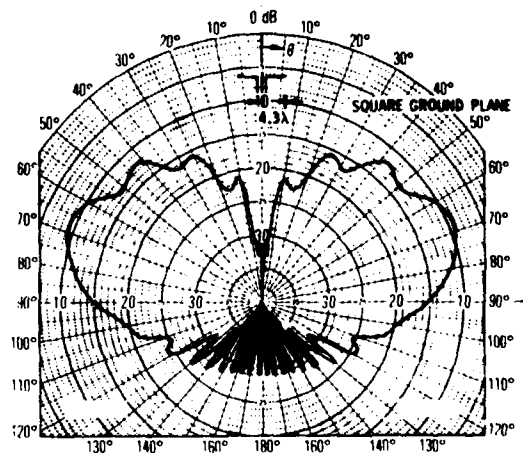
Fig. 7. Computed Pattern of Monopole   Fig. 8. Computed Pattern of Monopole
         over Circular Ground Plane   over Square Ground Plane

19

III. SUMMARY AND CONCLUSIONS

The OSU OSUPATT computer program was incorporated into our CDC 7600 computer. The computer code has the capability for the calculation of reflector antenna gain and patterns, including wide-angle sidelobes and backlobes, over a 80-dB dynamic range with reasonably good accuracy. The code accounts for strut and feed blockage and diffraction from the edge of the dish. We have subsequently added a circular polarization subroutine and a plot subroutine to the program.

The GTD was applied to the program for the computation of the diffraction from metal edges and of the radiation patterns of a monopole mounted over a circular or rectangular ground plane. It is shown that the diffraction from an edge can be reduced by the use of a rounded edge rather than a sharp edge if the region of interest is at least 30° into the shadow region. The validity of this diffraction-reduction technique was verified by experimental data. The monopole analysis can treat a wide variety of geometries and provides a method of assessing the diffraction distortions caused by finite size ground planes. The theoretical analyses performed to date have extended our in-house capabilities for the computation of antenna characteristics.

REFERENCES

1. S. H. Lee, R. C. Rudduck, C. A. Klein, and R. G. Kouyoumjian, A GTD
    Analysis of the Circular Reflector Antenna Including Feed and Strut
    Scatter, Report No. 4381-1, Ohio State University, Columbus (25 May
    1977).

2. S. Silver, Microwave Antenna Theory and Design, MIT Radiation Laboratory
    Series, Vol. 12, Chap. 6, McGraw-Hill Book Co. (1949).

3. S. H. Lee, R. C. Rudduck, and N. Wang, "Feed Strut Scattering Analysis
    for Wide Angle Sidelobes," 1979 IEEE International Antennas and
    Propagation Symposium Digest, Seattle, Wash., 18-22 June 1979, pp. 63-66.

4. R. G. Kouyoumjian, "Asymptotic High-Frequency Methods," Proc. IEEE, 53
    864-876 (August 1965).

5. R. G. Kouyoumjian, "The Geometrical Theory of Diffraction and Its
    Application," Topics in Applied Physics, Vol. 3, ed. R. Mittra, Numerical
    and Asymptotic Techniques in Electromagnetics, Springer-Verlag, New York,
    Heidelberg, Berlin (1975), pp. 166-213.

6. A. R. Lopez, "The Geometrical Theory of Diffraction Applied to Antenna
    Pattern and Impedance Calculations," IEEE Trans. on Antennas and Propag.
    AP-14, 40-45 (January 1966).

7. C. E. Ryan and L. Peters, "Evaluation of Edge-Diffracted Fields Including
    Equivalent Currents for the Caustic Regions," IEEE Trans. on Antennas and
    Propag. AP-17, 292-299 (May 1969).

LABORATORY OPERATIONS

The Laboratory Operations of The Aerospace Corporation is conducting experimental and theoretical investigations necessary for the evaluation and application of scientific advances to new military concepts and systems. Versatility and flexibility have been developed to a high degree by the laboratory personnel in dealing with the many problems encountered in the Nation's rapidly developing space systems. Expertise in the latest scientific developments is vital to the accomplishment of tasks related to these problems. The laboratories that contribute to this research are:

Aerophysics Laboratory: Aerodynamics; fluid dynamics; plasmadynamics; chemical kinetics; engineering mechanics; flight dynamics; heat transfer; high-power gas lasers, continuous and pulsed, IR, visible, UV; laser physics; laser resonator optics; laser effects and countermeasures.

Chemistry and Physics Laboratory: Atmospheric reactions and optical backgrounds; radiative transfer and atmospheric transmission; thermal and state-specific reaction rates in rocket plumes; chemical thermodynamics and propulsion chemistry; laser isotope separation; chemistry and physics of particles; space environmental and contamination effects on spacecraft materials; lubrication; surface chemistry of insulators and conductors; cathode materials; sensor materials and sensor optics; applied laser spectroscopy; atomic frequency standards; pollution and toxic materials monitoring.

Electronics Research Laboratory: Electromagnetic theory and propagation phenomena; microwave and semiconductor devices and integrated circuits; quantum electronics, lasers, and electro-optics; communication sciences, applied electronics, superconducting and electronic device physics; millimeter-wave and far-infrared technology.

Materials Sciences Laboratory: Development of new materials; composite materials; graphite and ceramics; polymeric materials; weapons effects and hardened materials; materials for electronic devices; dimensionally stable materials; chemical and structural analyses; stress corrosion; fatigue of metals.

Space Sciences Laboratory: Atmospheric and ionospheric physics, radiation from the atmosphere, density and composition of the atmosphere, auroras and airglow; magnetospheric physics, cosmic rays, generation and propagation of plasma waves in the magnetosphere; solar physics, x-ray astronomy; the effects of nuclear explosions, magnetic storms, and solar activity on the earth's atmosphere, ionosphere, and magnetosphere; the effects of optical, electromagnetic, and particulate radiations in space on space systems.

. . .

D
FI
8